ELSEVIER

Biochimica et Biophysica Acta 1474 (2000) 337–345

BIOCHIMICA ET BIOPHYSICA ACTA
BBA

www.elsevier.com/locate/bba

Spatiotemporal dynamics of fibrin formation and spreading of active thrombin entering non-recalcified plasma by diffusion

Yuliya V. Krasotkina *, Elena I. Sinauridze, Fazoil I. Ataullakhanov

Research Center for Hematology, Russian Academy of Medical Sciences, Novozykovskii pr. 4a, Moscow, 125167 Russia

Received 5 July 1999; received in revised form 20 January 2000; accepted 1 February 2000

Abstract

The spatiotemporal dynamics of clot growth was studied in non-stirred non-recalcified plasma where thrombin entered by diffusion. Under these conditions, the clot rapidly grew for 30–45 min and then stopped growing on reaching 0.4–0.5 mm in size. The dynamics of clot growth and its size almost did not depend on the thrombin concentration in the range from 50 to 400 nM. FITC-thrombin was shown to permeate the growing clot. The clot size in antithrombin-deficient plasma increases with decreasing antithrombin concentration, being 1.5 mm in the plasma depleted of antithrombin to 5% of its initial level. The data on the spatial distribution of amidolytic activity in the growth zone of the clot suggested that thrombin was not the sole source of this activity. Analysis showed that this additional activity arising during thrombin diffusion into plasma was largely accounted for by thrombin-α_2-macroglobulin complex.

Keywords: Blood coagulation; Clot growth dynamics; Thrombin; Citrate plasma; Fibrinogen

1. Introduction

Thrombin is the key enzyme of the coagulation cascade. At the final stage of coagulation, it converts fibrinogen into fibrin, which forms a hemostatic clot. However, the presence of active thrombin in the circulation may lead to life-threatening intravascular coagulation. Therefore, in order to reach effective hemostasis that is not followed by thrombosis, the terminal phases of coagulation must be precisely regulated. Within the body, coagulation is terminated through both activation of the protein C pathway, which stops thrombin generation, and inactivation of the generated thrombin by abundant plasma inhibitors, of which the most potent is antithrombin (AT).

The reactions of thrombin inhibition have been extensively studied in experimental systems with full stirring [1] in which all reagents are uniformly distributed over the entire sample volume, and, therefore, the rate of each individual reaction is the same at any point of the sample volume. However, within the body, coagulation is initiated at the surface of a damaged vessel and is strictly localized to the site of injury. This situation is characterized by extremely non-uniform spatial distribution of activated factors and their inhibitors. In [2], it was suggested that the dynamics of coagulation in spatially uniform and non-uniform environments differ qualitatively. Obviously, the spatial non-uniformity in concentrations of all participants is an important factor influencing the spatial organization of the reactions of thrombin inhibition [3].

In this study, the spatiotemporal dynamics of fibrin formation and thrombin inhibition were examined under conditions of thrombin diffusion into non-recalcified plasma. Our experimental system allowed the activated factors and their inhibitors to be distributed in space according to their concentration gradients. The absence of calcium ions precluded the activation of the coagulation cascade and the formation of additional amounts of thrombin from its plasma precursor. Therefore, this experimental model allowed the spatial effects of thrombin inhibition by pre-existing plasma inhibitors to be clearly revealed. Previously, in a similar experimental system, we observed the formation of clots of limited sizes and studied the dependencies of clot weight on the time of thrombin dif-

Abbreviations: AMC, 7-amino-4-methylcoumarin; AT, antithrombin; BOC-Ala-Pro-Arg-AMC, *t-N*-butoxycarbonyl-alanyl-prolyl-arginyl-7-amino-4-methylcoumarin; CPD, citrate–phosphate–dextrose solution; CPDA-1, citrate–phosphate–dextrose–adenine solution; DMSO, dimethyl sulfoxide; FITC, fluorescein isothiocyanate; PPP, platelet-poor plasma; PVC, polyvinyl chloride

* Corresponding author. Fax: +7-95-212-8870;
E-mail: julya@blood.ru

0304-4165/00/$ – see front matter
PII: S0304-4165(00)00019-2

fusion into plasma and on the concentration of exogenous thrombin [4]. In this study, we used the optical method to observe the geometry of a growing clot and the temporal evolution of the spatial distribution of amidolytic activity induced by thrombin diffusing into non-recalcified plasma.

2. Materials and methods

2.1. Materials

Platelet-poor plasma (PPP) was isolated from random-donor blood units stabilized with standard citrate anticoagulants CPD and CPDA-1 by centrifugation at $2400 \times g$ (22°C) for 20 min. The supernatant PPP contained less than 2×10^{10} platelets/l; the free calcium concentration ranged from 30 to 40 μM. The PPP was stored in individual PVC blood packs (Kompoplast-300, Russia) at room temperature for no longer than 72 h from the moment of blood collection. Experiments were performed on pooled PPP prepared every time immediately before the experiment from three or four individual PPP units.

Antithrombin-deficient plasma was prepared by immunoaffinity chromatography on goat antihuman antithrombin antibody-coupled CNBr-activated Sepharose 4B (Pharmacia, Sweden). The antithrombin concentration was determined by enzyme immunoassay [5]. The immunoadsorbed plasma was depleted of antithrombin by 95% or more after a single application of a 1-ml plasma aliquot to a column containing 0.5 ml of the immunoadsorbent.

Bovine thrombin (Merck, Germany) and human fibrinogen free of plasmin(ogen) were dissolved to desired concentrations in 50 mM imidazole buffer (pH 7.4), containing 145 mM NaCl and 5% human albumin for i.v. infusions (Bogdanov Institute of Blood Transfusion, Research Center for Hematology, Russian Academy of Medical Sciences, Russia).

Thrombin was conjugated to fluorescein isothiocyanate (FITC; Sigma, USA) at the Institute of Immunology (Ministry of Health, Moscow, Russia) according to the method described in [6].

A specific substrate for thrombin *t*-*N*-butoxycarbonyl-Ala-Pro-Arg-7-amino-4-methylcoumarin (BOC-Ala-Pro-Arg-AMC) [7] was synthesized at the Institute of Biological and Medical Chemistry (Russian Academy of Medical Sciences, Moscow, Russia). The substrate was stored as a 10-mM stock solution in DMSO (Merck, Germany) at −20°C until experiments.

Low-melting point agarose was purchased from Fluka (Germany), polyethylene glycol 6000 from Serva (Germany), and 7-amino-4-methylcoumarin (AMC) from Sigma (USA). Argatroban (Mitsubishi Chemical Corporation, Japan) was a kind gift from Dr. Jin Shiomura. All other reagents used were domestic products of the highest purity grade available.

2.2. Determination of thrombin activity

Thrombin activity was determined fluorometrically on a JY 3D instrument (Jobin Yvon, France) from the hydrolysis rate of BOC-Ala-Pro-Arg-AMC. Fluorescence of AMC was recorded using the excitation and emission wavelengths of 380 and 440 nm, respectively. Thrombin activity was calculated from the initial hydrolysis rates of the substrate and the kinetic constants $k_{cat} = 130\ s^{-1}$ and $K_m = 13$ μM for this reaction available from the literature [7]. The signals recorded were calibrated by comparison with the signal from 1 μM AMC in the same buffer.

2.3. Study of the spatiotemporal dynamics of coagulation

A special polystyrene chamber (Fig. 1A) was used to study the spatiotemporal dynamics of clot formation and changes in activity of the thrombin entering non-recalcified PPP or fibrinogen solution by diffusion. The chamber consisted of two compartments separated with a thin (8-μm) polyethylene terephthalate film with pores of 3-μm diameter (Joint Institute for Nuclear Research, Dubna, Moscow oblast, Russia). Each compartment was 300 μl in volume and 1 mm in height. In order to prevent distortion of the spatial distribution of coagulation factors caused by convection, melted agarose polymerizing at 36°C was added to the non-recalcified plasma supplemented with 100 μM Boc-Ala-Pro-Arg-AMC and preheated to 38°C. The final agarose concentration in plasma was 0.2%; all additions to the plasma accounted for no more than 4% of its volume. The agarose–plasma mixture was transferred to one of the compartments that was kept at room temperature and allowed to polymerize. The chamber was then placed in the thermostat of the experimental setup that was kept at 37°C throughout the experiment. Immediately before the experiment, the other compartment was filled with thrombin of the known concentration (in the range from 50 to 400 nM). The interval between the moment of filling the second compartment with thrombin and the start of recording was no more than 1.5 min.

Thrombin diffusing into the plasma compartment reacted with the fluorogenic substrate, giving rise to AMC. AMC fluorescence was continuously recorded at each point of the chamber. After being corrected for AMC diffusion, the fluorescence signal at each point reflected the amount of active thrombin present at this point.

The spatial AMC distributions were recorded using the computer-assisted laboratory setup shown in Fig. 1B. Light from (1) a mercury lamp passed through (2) an aqueous heat-blocking filter and a glass filter blocking visible part of the spectrum and impinged on (5) a semitransparent interference mirror that was placed in the light path so that (4) the chamber with plasma was illuminated from below. The filters and the mirror provided narrowband light with a maximum at 380 nm to excite AMC

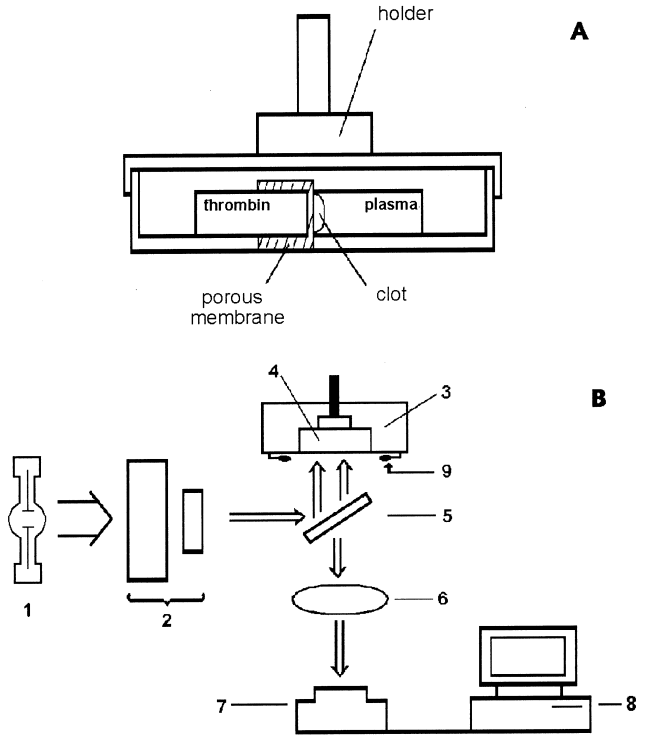

Fig. 1. Scheme of the laboratory set-up. (A) Scheme of the polystyrene chamber. (B) Scheme of the laboratory set-up: 1, mercury lamp; 2, light-blocking filters; 3, thermostat; 4, polystyrene chamber; 5, interference mirror; 6, optic focusing system; 7, CCD camera; 8, computer; and 9, diodes.

fluorescence. The maximum of AMC fluorescence is at 440 nm. The mirror was transparent at this wavelength. The fluorescence signal was recorded with (7) a digital CCD camera (Electrium, USA) mounted under the mirror. The image of an area measuring 9×6.5 mm (which could be chosen in any part of the polystyrene chamber) was transferred from the RGB matrix of the CCD camera to (8) the computer and displayed on the monitor screen. The data were recorded into files for the off-line analysis.

All images were processed under the assumption that they were symmetrical with respect to the normal to the membrane. This allowed us to consider the one-dimensional rather than two-dimensional distributions of AMC fluorescence along an arbitrary chosen perpendicular (scan line) to the membrane. To calibrate the AMC fluorescence signal, AMC at a known concentration was added to the plasma, and its image (calibration frame) was recorded. The calibration frame was used to normalize the fluorescence signals recorded during the experiment. The results were expressed in AMC concentration units. The spatial non-uniformity of UV illumination of the chamber was also eliminated by this calibration procedure. The first frame (background) was recorded immediately after the thrombin compartment of the chamber has been filled.

In some experiments, fibrinogen solutions were used instead of plasma. The experimental procedure was essentially the same as in experiments with plasma.

Thrombin diffusion was visualized using thrombin conjugated with FITC (a fluorescent label). Preliminary experiments showed that FITC produced no effect on thrombin activity. The procedure for recording FITC fluorescence was essentially the same as that for recording AMC fluorescence; only the filters (Fig. 1B, (2)) were changed to provide the excitation maximum of 490 nm.

Clot growth was monitored by the increase in light scattering. The chamber was illuminated from below using red light diodes (Fig. 1B, (9)). No calibration was performed; therefore, the results were expressed in arbitrary units, rather than in fibrin concentration units.

The image processing in analysis of the AMC profiles was performed using the software package supplied with the CCD-camera and the Microsoft Origin graphical processor.

2.4. Mathematical model

The model was constructed to describe and analyze the spatial AMC and fibrin distributions observed under the experimental conditions used. The model involved equations for the following biochemical reactions:

$$T + Fg \Leftrightarrow TFg \Rightarrow T + Fn \quad (1)$$

$$T + Fn \Leftrightarrow TFn \quad (2)$$

$$TFn + Fg \Leftrightarrow TFnFg \Rightarrow TFn + Fn \quad (3)$$

$$T + I_1 \Leftrightarrow TI_1 \quad (4)$$

$$TFn + I_1 \Leftrightarrow TFnI_1 \quad (5)$$

$$T + I_2 \Leftrightarrow TI_2 \quad (6)$$

$$T + S \Leftrightarrow TS \Rightarrow T + AMC \quad (7)$$

$$TFn + S \Leftrightarrow TFnS \Rightarrow TFn + AMC \quad (8)$$

$$TI_2 + S \Leftrightarrow TI_2S \Rightarrow TI_2 + AMC \quad (9)$$

here, T denotes thrombin; Fg and Fn are fibrinogen and fibrin, respectively; I_1 stands for the inhibitors of thrombin (antithrombin, or argatroban), and I_2 stands for α_2-macroglobulin; S is the fluorogenic substrate; AMC is its cleavage product; TFg, TI_1, TI_2, and TS denote the complexes of thrombin with fibrinogen, inhibitors, or fluorogenic substrate, respectively; TI_2S is thrombin-α_2-macroglobulin-fluorogenic substrate complex; and TFn, TFnFg, $TFnI_1$, and TFnS denote thrombin bound with fibrin and the complexes thereof with fibrinogen, inhibitors (antithrombin or argatroban), or fluorogenic substrate, respectively.

In the model, thrombin adsorbed to fibrin was assumed to retain the ability to interact with fibrinogen, inhibitors (excluding α_2-macroglobulin), and fluorogenic substrate.

Table 1
Kinetic constants used in analysis of the mathematical model

Reaction	Kinetic constants	Reference
$T+Fg \Leftrightarrow TFg \Rightarrow T+Fn$	$k_{cat}^{F} = 5040\ min^{-1}$; $K_m^{F} = 7.2\ \mu M$	[11]
$TFn+Fg \Leftrightarrow TFnFg \Rightarrow TFn+Fn$	$k_{cat}^{F} = 5040\ min^{-1}$; $K_m^{F} = 7.2\ \mu M$	
$T+Fn \Leftrightarrow TFn$		[12]
For non-crosslinked fibrin	$k_a = 1.3\times10^{-3}\ \mu M^{-1}\ min^{-1}$; $k_d = 4300\ min^{-1}$; $K_a = 4.6\times10^{-1}\ \mu M^{-1} = 4.6\times10^{5}\ M^{-1}$	
For crosslinked fibrin	$k_a = 1\times10^{-3}\ \mu M^{-1}\ min^{-1}$; $k_d = 2170\ min^{-1}$; $K_a = 3\times10^{-1}\ \mu M^{-1} = 3\times10^{5}\ M^{-1}$	
$T+I_1 \Leftrightarrow TI_1$		
For antithrombin	$k_{i1} = 1\ \mu M^{-1}\ min^{-1}$; $k_{-i1} = 1\times10^{-4}\ min^{-1}$; $K_d = 1\times10^{-4}\ \mu M = 10^{-10}\ M$	[11,13,14]
For argatroban	$k_{i1} = 1\ \mu M^{-1}\ min^{-1}$; $k_{-i1} = 1.9\times10^{-2}\ min^{-1}$; $K_d = 1.9\times10^{-2}\ \mu M = 19\times10^{-9}\ M$	[15]
$T+I_2 \Leftrightarrow TI_2$		
For α_2-macroglobulin (α_2MG)	$k_{i2} = 0.1\ \mu M^{-1}\ min^{-1}$; $k_{-i2} = 1\times10^{-4}\ min^{-1}$; $K_d = 1\times10^{-3}\ \mu M = 1\times10^{-9}\ M$	
$TFn+I_1 \Leftrightarrow TFnI_1$		
For antithrombin	$k_{i3} = 0.6\ \mu M^{-1}\ min^{-1}$; $k_{-i3} = 1\times10^{-4}\ min^{-1}$; $K_d = 1.67\times10^{-4}\ \mu M = 1.67\times10^{-10}\ M$	[11]
For argatroban	$k_{i3} = 1\ \mu M^{-1}\ min^{-1}$; $k_{-i3} = 1.9\times10^{-2}\ min^{-1}$; $K_d = 1.9\times10^{-2}\ \mu M = 19\times10^{-9}\ M$	[16]
$T+S \Leftrightarrow TS \Rightarrow T+AMC$	$k_{cat}^{S} = 7800\ min^{-1}$; $K_m^{S} = 13\ \mu M$	[7]
$T\alpha_2MG+S \Leftrightarrow T\alpha_2MGS \Rightarrow T\alpha_2MG+AMC$	$k_{cat}^{S1} = 4680\ min^{-1}$; $K_m^{S1} = 13\ \mu M$	[17]
$TFn+S \Leftrightarrow TFnS \Rightarrow TFn+AMC$	$k_{cat}^{S1} = 4680\ min^{-1}$; $K_m^{S1} = 13\ \mu M$	

All indicated above reactions may be described by the following set of differential equations:

$$\frac{dT}{dt} = D_T\cdot\frac{\partial^2 T}{\partial x^2} - k_a\cdot T\cdot Fn + k_d\cdot TFn - k_{i1}\cdot T\cdot I_1 + k_{-i1}\cdot TI_1 - k_{i2}\cdot T\cdot I_2 + k_{-i2}\cdot TI_2 \quad (10)$$

$$\frac{dI_1}{dt} = D_I\cdot\frac{\partial^2 I_1}{\partial x^2} - k_{i1}\cdot T\cdot I_1 + k_{-i1}\cdot TI_1 - k_{i3}\cdot TFn\cdot I_1 + k_{-i3}\cdot TFnI_1 \quad (11)$$

$$\frac{dI_2}{dt} = -k_{i2}\cdot T\cdot I_2 + k_{-i2}\cdot TI_2 \quad (12)$$

$$\frac{dTI_1}{dt} = D_{TI}\cdot\frac{\partial^2 TI_1}{\partial x^2} + k_{i1}\cdot T_1\cdot I_1 - k_{-i1}\cdot TI_1 \quad (13)$$

$$\frac{dTI_2}{dt} = k_{i2}\cdot T\cdot I_2 - k_{-i2}\cdot TI_2 \quad (14)$$

$$\frac{dTFn}{dt} = k_a\cdot T\cdot Fn - k_d\cdot TFn - k_{i3}\cdot TFn\cdot I_1 + k_{-i3}\cdot TFnI_1 \quad (15)$$

$$\frac{dTFnI_1}{dt} = k_{i3}\cdot TFn\cdot I_1 - k_{-i3}\cdot TFnI_1 \quad (16)$$

$$\frac{dS}{dt} = D_S\cdot\frac{\partial^2 S}{\partial x^2} - \frac{k_{cat}^{S}\cdot T\cdot S}{K_m^{S}+S} - \frac{k_{cat}^{S1}\cdot(TFn+TI_2)\cdot S}{K_m^{S1}+S} \quad (17)$$

$$\frac{dAMC}{dt} = D_{AMC}\cdot\frac{\partial^2 AMC}{\partial x^2} + \frac{k_{cat}^{S}\cdot T\cdot S}{K_m^{S}+S} + \frac{k_{cat}^{S1}\cdot(TFn+TI_2)\cdot S}{K_m^{S1}+S} \quad (18)$$

$$\frac{dFn}{dt} = \frac{k_{cat}^{F}\cdot(T+TFn)\cdot Fg}{K_m^{F}+Fg} - k_a\cdot T\cdot Fn + k_d\cdot TFn \quad (19)$$

$$\frac{dFg}{dt} = -\frac{k_{cat}^{F}\cdot(T+TFn)\cdot Fg}{K_m^{F}+Fg} \quad (20)$$

Here, D_T, D_I, D_{TI}, D_S, and D_{AMC} are the diffusion coefficients of the respective components of the system. Their values were chosen according to the molecular weights of the components using the data from [8]. Specifically, the diffusion coefficients for thrombin and antithrombin, were set to 0.003 mm^2/min; the values of 0.0024, 0.015, 0.015, and 0.035 mm^2/min were used for thrombin–antithrombin complex, substrate S, argatroban, and AMC, respectively. We neglected the diffusion of fibrin, fibrinogen, α_2-macroglobulin, and their complexes, as their molecular weights are much greater than the molecular weights of other components of the system.

Interaction of thrombin, whether free or fibrin-bound, with inhibitors was considered to be a reversible second-order reaction. Interactions of thrombin, fibrin-bound thrombin, or α_2-macroglobulin–thrombin complex with fibrinogen and/or the substrate were described by the Michaelis–Menten equations.

The set of equations was solved by the first-order Euler method using the explicit difference scheme [9] or the adaptive Runge–Kutta method of the approximation order of 2(3) [10]. Both methods led to similar results.

The kinetic constants used in computations are shown in Table 1.

3. Results

3.1. Diffusion of fluorescently labeled thrombin in buffered saline or plasma

Diffusion of thrombin through a membrane was studied using purified thrombin labeled with fluorescein isothiocyanate (FITC). The spatial profiles of FITC-thrombin diffusing through a membrane into imidazole-buffered saline and non-recalcified plasma are shown in Fig. 2a and b, respectively. In plasma, a clot grew on the membrane,

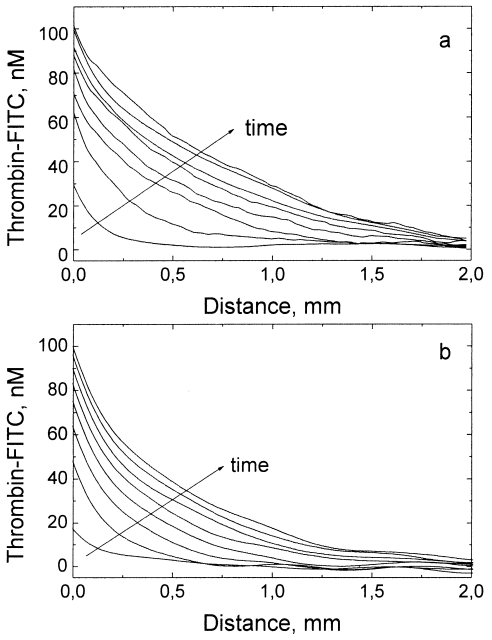

Fig. 2. Concentration profiles of FITC-thrombin (200 nM) diffusing into (a) 50 mM imidazole buffer containing 145 mM NaCl and 5% human albumin for i.v. infusions or (b) non-recalcified plasma. The first curve was recorded 2 min after the start of the experiment; all other curves were recorded every 15 min after the start of the experiment.

whereas in buffer, the membrane remained free of clot growth throughout the experiment. In this and other figures, the curves show how the recorded parameter changes in space along an arbitrarily chosen scan line in the direction perpendicular to the membrane. Each Figure shows a family of curves recorded along the same line at various times from the start of the experiment. The diffusion profiles of FITC-thrombin are similar in buffer and plasma (Fig. 2a,b). By the end of the experiment (2 h), thrombin spread over a distance of about 1.5–2 mm.

3.2. *Dynamics of clot growth induced by thrombin diffusing into non-recalcified plasma: effects of various thrombin concentrations*

Thrombin entering the plasma compartment induced the formation of a solid fibrin clot, i.e. the structure denser than the surrounding plasma. Light scattering increased in the area of clot formation above the background level observed initially in the plasma (this initial value of light scattering was taken as zero). The spatial profiles of light scattering observed in plasma for the concentrations of diffusing thrombin of 50 and 400 nM are shown in Fig. 3a and b, respectively. In both cases, the area of increased scattering was localized to the membrane and had clear-cut edges that characterized the clot shape. Two stages were evident in the dynamics of changes in the light scattering by the clot. At the first stage, which was 30–45 min long, the intensity of light scattering by the rapidly growing clot increased. The area of increased light scattering expanded to a distance of 0.3–0.5 mm from the membrane. During the subsequent 1.5 h, the spatial boundary of the clot remained almost unchanged; however, the intensity of light scattered by the area occupied by the clot

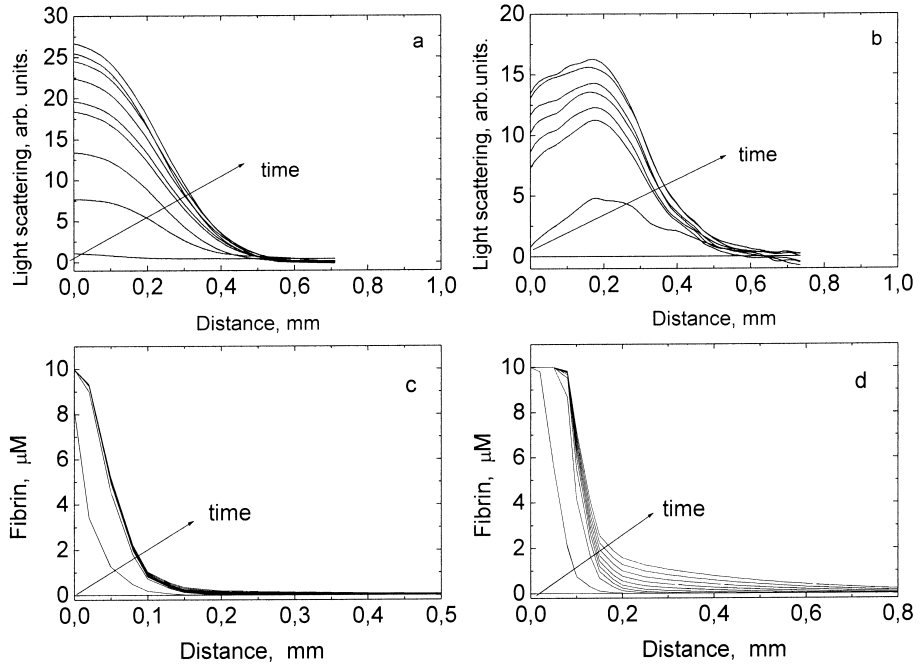

Fig. 3. Clot growth induced by thrombin diffusing into non-recalcified plasma: (a,b) light scattering profiles and (c,d) calculated fibrin profiles for thrombin concentrations of (a,c) 50 and (b,d) 400 nM. The first curve was recorded 2 min after the start of the experiment; all other curves were recorded every 15 min after the start of the experiment.

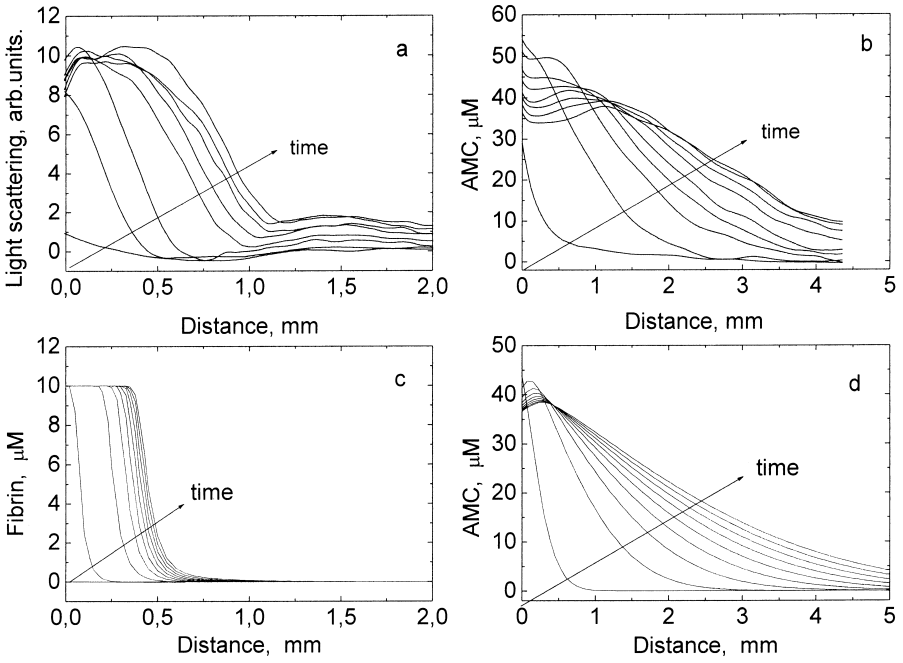

Fig. 4. Clot growth and AMC formation induced by 200 nM thrombin diffusing into non-recalcified plasma containing only 5% of the initial antithrombin: (a) experimental light scattering profiles; (b) experimental AMC concentration profiles; (c) fibrin profiles calculated theoretically; and (d) theoretical AMC concentration profiles. The first curve was recorded 2 min after the start of the experiment; all other curves were recorded every 15 min after the start of the experiment.

continued to increase, but at a rate considerably lower than the rate observed during the first minutes of clot growth. As evident from comparison of Fig. 3a and b, the dynamics of clot formation and its geometric characteristics only weakly depended on the thrombin concentration in a broad range.

In plasma depleted of AT to 5% of its initial level, clots did not stop growing throughout the experiment (Fig. 4a).

3.3. Dynamics of AMC formation in plasma or fibrinogen solutions

Active thrombin was visualized by its reaction with a specific substrate, giving rise to the fluorescent product -7-amino-4-methylcoumarin. Figure 5a shows the AMC concentration profiles for 200 nM of thrombin diffusing into plasma. As in the previous case, two different stages are evident in the generation of AMC in plasma. During the first 15–30 min, the AMC concentration increased at each point of the scan line, with the formation of a maximum near the membrane. During the subsequent 1.5 h, this concentration maximum began to move away from the membrane and progressively decreased in amplitude. The distance that the AMC concentration maximum run away from the membrane over the time of the experiment was 1.0–1.5 mm. Fig. 4b shows the AMC profiles observed in plasma depleted of AT to 5% of its initial concentration. Evidently, AT depletion did not change the AMC concentration profiles: the profiles observed before and after depletion were similar, both qualitatively and quantitatively. We had no purified AT at our disposal; therefore, to simulate the effect of pre-existing inhibitors on the dynamics of active thrombin spreading, we supplemented 4 mg/ml fibrinogen with argatroban, a synthetic inhibitor of thrombin [15], to a final concentration of 5 μM. Fig. 6 shows the AMC concentration profiles for 200 nM of thrombin diffusing into fibrinogen solution containing argatroban. Evidently, the AMC concentration continuously increased at each point over the 2 h of the experiments. The profiles exhibited no running maximum.

3.4. Theoretical simulation of the fibrin and AMC profiles in the system under study

Using the model described above, we calculated the fibrin and AMC distributions for thrombin (50–400 nM) diffusion into either: (1) 10 μM (4 mg/ml) fibrinogen containing 5 μM argatroban; or (2) 10 μM fibrinogen containing 5 μM α_2-macroglobulin and 3.0 or 0.15 μM AT.

The initial concentration of the fluorogenic substrate for thrombin was set to 100 μM, as in experiments.

As evident from the fibrin profiles (Fig. 3c,d) calculated for thrombin diffusion into fibrinogen solution containing 5 μM α_2-macroglobulin and 3.0 μM AT, which may be considered as an analog of the whole plasma, the clot would grow for 15–45 min and then stop growing. Its linear size would be 0.3–0.8 mm, depending on the thrombin concentration. The dynamics of clot formation corresponds to the dynamics observed in the experiments with plasma (Fig. 3a,b).

The theoretical profiles for fibrin were also calculated for thrombin diffusion into fibrinogen solution containing 5 μM α_2-macroglobulin and 0.15 μM AT, which may be considered as an analog of the AT-depleted plasma (Fig. 4c).

The model and experimental data on the AMC distributions are in a good qualitative agreement for thrombin diffusion into solution of purified fibrinogen containing 5 μM argatroban (Fig. 6).

Unlike the fibrin profiles, the AMC profiles calculated for fibrinogen solution containing 5 μM α_2-macroglobulin and 3.0 μM AT differ qualitatively from the profiles observed in the experimental plasma (Fig. 5b).

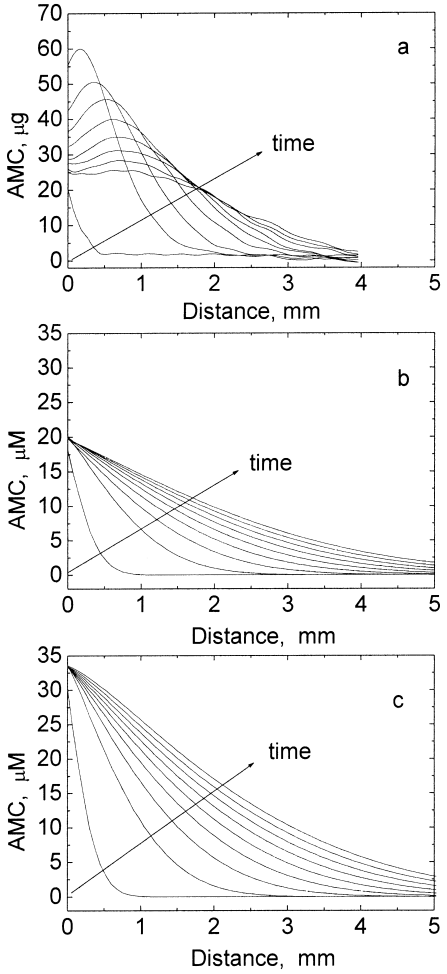

Fig. 5. AMC concentration profiles in non-recalcified plasma where thrombin (200 nM) is allowed to diffuse: (a) experimental data and the data simulated using the model constructed under assumption that the fluorogenic substrate is (b) not hydrolyzed or (c) hydrolyzed by thrombin–α_2-macroglobulin complex with a rate constant set to be 0.6 of the constant for free thrombin. The fluorogenic substrate concentration was 100 μM. The first curve was recorded 2 min after the start of the experiment; all other curves were recorded every 15 min after the start of the experiment.

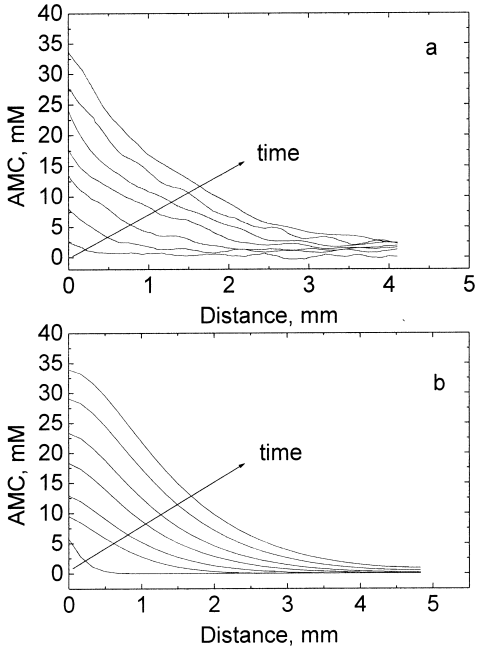

Fig. 6. AMC formation induced by thrombin diffusing into 4 mg/ml fibrinogen containing 5 μM argatroban: (a) experimental and (b) theoretical AMC concentration profiles for thrombin concentration of 200 nM. The constant of thrombin-argatroban complex dissociation in the model was set to 19 nM. The fluorogenic substrate concentration was 100 μM. The first curve was recorded 2 min after the start of the experiment; all other curves were recorded every 15 min after the start of the experiment.

4. Discussion

By studying the dynamics of clot growth upon thrombin diffusion in the non-stirred citrated plasma, we found that the clot rapidly grew for the first 30–45 min, increasing in size up to 0.4–0.5 mm, and then stopped growing for the subsequent 1.5 h (Fig. 3a,b). Interestingly, the clot size almost did not depend on the concentration of diffusing thrombin in the range from 50 to 400 nM. This finding is consistent with our previous data described in [4], in which in a similar experimental system, the clot stopped growing after a certain moment, and its weight slightly depends on the concentration of thrombin. The gradually increased intensity of light scattering inside the clot should non-linearly depend on the extent of fibrin polymerization and crosslinking. Therefore the intensity of light scattering cannot be easily interpreted in terms of fibrin concentration.

In diffusion experiments with FITC-thrombin, its spatial profiles in buffer and plasma were very similar (Fig. 2a,b), suggesting that in plasma, a clot growing on the membrane does not restrict diffusion of the enzyme molecules. The diffusion experiments with FITC-thrombin showed that it ran a distance 3–4 times greater than the characteristic clot size. During incubation, thrombin might be converted into γ-thrombin lacking clotting activity towards fibrinogen. However, this process is known to be very slow in the absence of specially added proteases [18,19].

Therefore, only a small amount of γ-thrombin could be formed over a period of 2 h (the maximum duration of our experiments). Most likely, the difference between the clot size and the distance over which thrombin spread by diffusion is accounted for by the formation of thrombin–inhibitor complexes.

In systems with full stirring, fibrin binds up to 30% of the total thrombin [12]. Therefore, we expected that, in spatially distributed systems, thrombin binding to fibrin might significantly affect thrombin diffusion through the clot. The adsorption was introduced into the model using the literature data [12]. The fibrin profiles in plasma calculated with the allowance for thrombin adsorption to fibrin are presented in Fig. 3c,d. In the model, clot growth stops in some 30 min after the start of diffusion. The higher the initial concentration of diffusing thrombin, the larger the final clot size. We varied the initial thrombin concentration from 50 to 400 nM; correspondingly, the clot size ranged from 0.3 to 0.8 mm. The calculated clot size only roughly corresponds to the clot size observed in experiments with thrombin diffusion into plasma (Fig. 3a,b). The fact that AT was far in excess of thrombin can explain why the enzyme permeating into plasma was rapidly inactivated and why the rate of the process only slightly depended on the thrombin concentration in the tested range (50–400 nM). The clots observed in the plasma depleted of AT to 5% of the initial level were significantly greater in size (Fig. 4a). This increase is well predictable by the proposed mathematical model (Fig. 4c).

In plasma thrombin binding to fibrin ($K_a = 3 \times 10^5$ M^{-1}) is less pronounced than it binding to AT ($K_a = 10^{10}$ M^{-1}). Therefore we suggest that adsorption of thrombin to fibrin had only little effect on the experimental clot size. Similar diffusion profiles of FITC-thrombin in plasma and buffer (i.e. in presence and absence of a clot, respectively; cf. Fig. 2b and a), as well as along duration of clot growth in plasma containing only 5% of the normal AT activity (Fig. 4a), in which clot grew to a larger size than in normal plasma, also suggest that adsorption of thrombin to fibrin could not have a profound effect on the spatial dynamics of clot growth.

Therefore, we may suggest that the presence of efficient inhibitors of thrombin (first and foremost AT) in non-recalcified plasma is the main factor responsible for the termination of clot growth in our experiments.

The spatial dynamics of active thrombin distribution was derived from changes in the concentration profiles of AMC, a hydrolysis product of the substrate specific for thrombin. The changes in the thrombin amidolytic activity profiles were also calculated by using the proposed mathematical model. As is evident from Fig. 5, the theoretical and experimental curves differ qualitatively. First, the amplitude of the experimental curves was always greater than the amplitude of the model curves (Fig. 5a,b). Second, in the experiments, a maximum of AMC concentration was formed near the membrane and moved away from it, progressively decreasing in amplitude. Therewith, the model successfully simulates the experimental AMC profiles in argatroban-containing fibrinogen solution (cf. Fig. 6a,b).

To explain the discrepancy between the model and experimental data, we have to suggest that an enzyme other than thrombin arose in the plasma and that this enzyme was capable of cleaving the fluorogenic substrate. The most probable candidate to play this role is thrombin–α_2-macroglobulin complex. Being inactive towards fibrinogen, thrombin in complex with α_2-macroglobulin is known to retain activity towards some of its low-molecular-weight substrates [17]. Obviously, this complex could contribute to the amidolitic activity observed in the plasma throughout the experiment. Although no data are available in the literature concerning the substrate we used, it is not unlikely that such activity exists. Using the model, we calculated the AMC concentration profiles in plasma, assuming that thrombin–α_2-macroglobulin complex cleaved the substrate and that the rate constant for this reaction was proportional to that obtained with substrate S2238 [17] (Fig. 5c). Despite the fact that the agreement with experimental profiles is more successful in this case, the formation of the running AMC maximum with progressively decreasing amplitude remains unexplained. The high molecular weight of this complex implies that its spatial diffusion is too slow to provide the observed displacement (1.0–1.5 mm) of the AMC concentration maximum over the time of the experiment (2 h).

A possible source of thrombin-induced amidolytic activity towards the fluorogenic substrate in plasma may be some plasma enzymes activated by thrombin. For instance, thrombin is known to activate protein C [20] and perhaps factor XI [21,22]. However, the rate constant for cleaving the fluorogenic substrate used with activated protein C is too low [7] to give rise to the running AMC maximum in the system. The issue of whether thrombin activates factor XI in plasma remains a matter of controversy [21–24]. Anyway, the rate of this reaction in the presence of fibrinogen is also very low [24]. As it was mentioned above, the formation of γ-thrombin (the form of thrombin without clotting activity, but capable of cleaving small substrates) also could not account for the extra amidolytic activity because of the low rate of thrombin conversion under our experimental conditions [18,19]. In addition, γ-thrombin is inhibited by AT as efficiently as α-thrombin [25].

Therefore, now we are uncertain what is the mechanism responsible for the observed decrease in the intensity of AMC fluorescence near the membrane and the formation of its maximum in the plasma. An explanation may be proposed within the framework of the autowave hypothesis of coagulation [2,3,26]. In this hypothesis, thrombin was suggested to initiate the production of its own inhibitor. The concentration wave of the inhibitor runs after the thrombin wave. The interaction of the two waves may

result in the formation of the AMC concentration maximum, which we observed in the experiment.

Acknowledgements

We are grateful to Dr. Jin Shiomura (Mitsubishi Chemical Corporation, Japan) for his kind gift of argatroban, Dr. A.V. Pichugin (The Institute of Immunology, Ministry of Health, Russia) for preparation of FITC-thrombin, and Dr. R.I. Volkova for excellent editorial assistance. This study was supported in part by the Russian Foundation for Basic Research (Project 97-04-49223).

References

[1] J. Jesty, Y. Nemerson, The pathways of blood coagulation, in: E. Beutler, M.A. Lichtman, B.S. Coller, T.J. Kipps (Eds.), Williams Hematology, 5th edn., McGraw-Hill Health Professions Division, New York, 1995, pp. 1227–1239.
[2] F.I. Ataullakhanov, G.T. Guria, Spatial aspects of the dynamics of blood coagulation: I. Hypothesis, Biophysics 39 (1994) 91–97.
[3] F.I. Ataullakhanov, G.T. Guria, A.Yu. Safroshkina, Spatial aspects of the dynamics of blood coagulation: II. Phenomenological model, Biophysics 39 (1994) 99–108.
[4] E.I. Sinauridze, R.I. Volkova, Yu.V. Krasotkina, V.I. Sarbash, F.I. Ataullakhanov, Dynamics of clot growth induced by thrombin diffusing into non-stirred citrate human plasma, Biochim. Biophys. Acta 1425 (1998) 607–616.
[5] A.V. Navdaev, Characterization of in vitro fibrin clot growth in human plasma, Cand. Sc. (Biol.) dissertation, Moscow: Cardiology Research Complex, 1997, 48–49.
[6] L. Hudson, T.C. Hay, Practical Immunology, 3rd edn., Blackwell Scientific, Oxford, 1989, pp. 34–35.
[7] S. Kawabata, T. Miura, T. Morita, H. Kato, K. Fujikawa, S. Iwanaga, K. Takada, T. Kimura, S. Sakakibara, Highly sensitive peptide-4-methylcoumaryl-7-amide substrates for blood-clotting proteases and trypsin, Eur. J. Biochem. 172 (1988) 17–25.
[8] A.G. Marshal, Biological Chemistry: Principles, Technics, and Applications, John Wiley and Sons, New York, 1978, p. 159.
[9] S.J. Farlow, Partial Differential Equations for Scientists and Engineers, John Wiley and Sons, New York, 1982, pp. 283–295.
[10] G. Hall, J.M. Watt (Eds.), Modern Numerical Methods for Ordinary Differential Equations, Clarendon Press, Oxford, 1976, pp. 76–85.
[11] M.C. Naski, J.A. Shafer, A kinetic model for the α-thrombin-catalyzed conversion of plasma level of fibrinogen to fibrin in the presence of antithrombin III, J. Biol. Chem. 266 (1991) 13003–13010.
[12] C.Y. Lie, K.L. Kaplan, A.H. Markowitz, H.L. Nossel, The binding of thrombin to fibrin, J. Biol. Chem. 254 (1979) 10421–10425.
[13] J. Jesty, The kinetics of formation and dissociation of the bovine thrombin–antithrombin complex, J. Biol. Chem. 254 (1979) 10044–10050.
[14] A. Danielson, J. Bjork, Slow, spontaneous dissociation of the antithrombin–thrombin complex produces a proteolytically modified form of the inhibitor, FEBS Lett. 119 (1980) 241–244.
[15] R. Kikumoto, Y. Tamao, T. Tezuka, S. Tonomura, H. Hara, K. Ninomiya, A. Hijikata, S. Okamoto, Selective inhibition of thrombin by (2R,4R)-4-methyl-1-[N^2-[(3-methyl-1,2,3,4-tetrahydro-8-quinolinyl)sulfonyl]-L-arginyl)]-2-piperidinecarboxylic acid, Biochemistry 23 (1984) 85–90.
[16] C.N. Berry, C. Girardot, C. Lecoffre, C. Lunven, Effects of the synthetic thrombin inhibitor argatroban on fibrin- or clot-incorporated thrombin: comparison with heparin and recombinant hirudin, Thromb. Haemost. 72 (1994) 381–386.
[17] H. Kessels, G. Willems, H.C. Hemker, Analysis of thrombin generation in plasma, Comput. Biol. Med. 24 (1994) 277–288.
[18] J.W. Fenton, B.H. Landis, D.A. Walz, J.S. Finlayson, in: R.L. Lundblad, J.W. Fenton, K.G. Mann (Eds.), Chemistry and Biology of Thrombin, Ann Arbor Science, Ann Arbor, 1977, pp. 43–70.
[19] J.P. Boissel, B. Le Bonniec, M.J. Rabiet, D. Labie, J. Elion, Covalent structures of beta and gamma autolytic derivates of human alpha thrombin, J. Biol. Chem. 259 (1984) 5691–5697.
[20] F.J. Walker, P.J. Fay, Regulation of blood coagulation by the protein C system, FASEB J. 6 (1992) 2561–2567.
[21] D. Gailani, G.J. Broze Jr., Factor XII-independent activation of factor XI in plasma effects of sulfatides on tissue factor-induced coagulation, Blood 82 (1993) 813–819.
[22] P.A. von dem Borne, J.C. Meijers, B.N. Bouma, Feedback activation of factor XI by thrombin in plasma results in additional formation of thrombin that protects fibrin clots from fibrinolysis, Blood 86 (1995) 3035–3042.
[23] T. Brunnee, C. La Porta, S.R. Reddigari, V.M. Salerno, A.P. Kaplan, M. Silverberg, Activation of factor XI in plasma is dependent on factor XII, Blood 81 (1993) 580–586.
[24] C.F. Scott, R.W. Colman, Fibrinogen blocks the autoactivation and thrombin-mediated activation of factor XI on dextran sulfate, Proc. Natl. Acad. Sci. USA 89 (1992) 11189–11193.
[25] A. Bezeaud, M.-H. Denninger, M.-C. Guillin, Interaction of human α-thrombin and γ-thrombin with antithrombin III, protein C and thrombomodulin, Eur. J. Biochem. 153 (1985) 491–496.
[26] F.I. Ataullakhanov, G.T. Guria, V.I. Sarbash, R.I. Volkova, Spatiotemporal dynamics of clotting and pattern formation in human blood, Biochim. Biophys. Acta 1425 (1998) 453–468.